1 Three Billion Year Secular Evolution of the Triple Oxygen Isotope Composition of
2 Marine Chert

3 Justin A. Hayles[a]*, Laurence Y. Yeung[a], Martin Homann[b], Asmita Banerjee[a], Hehe Jiang[a], Bing Shen[c], Cin-Ty Lee[a]

4 [a]Department of Earth, Environmental and Planetary Sciences, Rice University, United States

5 [b] European Institute for Marine Studies, CNRS-UMR6538 Laboratoire Géosciences Océan,
6 Technopôle Brest-Iroise, Place Nicolas Copernic, 29280 Plouzané, France

7 [c]School of Earth and Space Sciences, Peking University, Beijing, China

8

9 * Corresponding author: justin.a.hayles@rice.edu

10

11 **Keywords:** Archean, chert, triple-oxygen-isotopes, marine silica
12

13 **Highlights:**

14 • Chert samples from the last 3.4 Gyr yield a secular evolution of $^{18}O/^{16}O$ and $^{17}O/^{16}O$

15 • Cherts since the Ordovician formed in water with $^{18}O/^{16}O$ and $^{17}O/^{16}O$ close to modern
16 seawater

17 • Precambrian cherts formed in different fluids or in different diagenetic environments
18

19

20 **Abstract:** The $^{18}O/^{16}O$ ratios of ancient marine minerals show a puzzling increase over geologic

21 time. Long-term changes in temperature, seawater $^{18}O/^{16}O$ ratios, and post-depositional

22 overprinting can all explain this trend, but few tracers can distinguish between these scenarios.

23 Here, we report high-precision $^{18}O/^{16}O$ and $^{17}O/^{16}O$ ratios of cherts through 3.4 Ga of Earth's

24 history. We find that Phanerozoic cherts are consistent with having formed in porewaters that are

25 isotopically indistinguishable from modern (ice-free) seawater. In contrast, Precambrian cherts

26 require either formation in waters isotopically distinct from Phanerozoic seawater, or a different

27 mode of formation. If the early diagenetic formation pathway of Precambrian cherts resembles that

28 of Phanerozoic cherts, and the Precambrian cherts are unaltered, then the results would imply that

29 the oxygen-isotope composition of seawater has evolved on billion-year timescales before

30 reaching its present composition by the Ordovician. Under this interpretation it is estimated that

31 seawater had $\delta'^{18}O < -11‰$ at 3.41 Ga, with surface temperatures $< 34°C$. Although this scenario

32 provides the simplest explanation for the observed $^{18}O/^{16}O$ trend of marine minerals, other

33 scenarios which do not require a secular change in seawater $^{18}O/^{16}O$ cannot be ruled out.

34

35

1.1 Introduction:

36

37   The oxygen isotope composition of seawater is buffered over geologic time by a balance

38   of high- and low-temperature interactions with the silicate Earth (Gregory and Taylor, 1981;

39   Muehlenbachs, 1998; Muehlenbachs and Clayton, 1976). These interactions have likely confined

40   the $^{18}O/^{16}O$ ratio in seawater to within a small range over the Phanerozoic (i.e. linearized notation:

41      $\delta'^{18}O = \ln[\delta^{18}O+1] = 0 \pm 2‰$ relative to VSMOW) (Coogan et al., 2019; Cummins et al., 2014;

42   Henkes et al., 2018). High-temperature interactions, such as those at seafloor hydrothermal

43   systems, tend to increase seawater $\delta'^{18}O$ values, while low-temperature interactions with oceanic

44   and continental crust tend to lower seawater $\delta'^{18}O$ values. Yet, details of how this seawater

45   buffering system operated for early Earth are unknown. The evolution of seawater $\delta'^{18}O$ may offer

46   clues to the evolution of the solid Earth over geologic time (Jaffrés et al., 2007; Kasting et al.,

47   2006). Changing subaerial exposure of mid-ocean ridges, penetration depths of seafloor

48   hydrothermal circulations, effective seafloor spreading rates, and the spatial extent of volcanic

49   plateaus can all affect seawater $\delta'^{18}O$ values by altering the proportions of high- and low-

50   temperature water-rock interactions at the global scale (Jaffrés et al., 2007; Kamber, 2010; Kasting

51   et al., 2006).

52   Compilations of data for marine carbonates, phosphates, shales and cherts all show a

53   secular increase in $\delta'^{18}O$ values over Earth history (Bindeman et al., 2016; Levin et al., 2014;

54   Veizer et al., 1997). The oldest minerals show $\delta'^{18}O$ values that are as much as 15‰ lower than

55   their modern equivalents. While a secular evolution of seawater $\delta'^{18}O$ can explain this trend, the

56   explanation is not unique: the $\delta'^{18}O$ data are also compatible with scenarios invoking ≥70°C Earth-

57   surface cooling since the Archean (Knauth and Epstein, 1976; Knauth and Lowe, 2003; Levin et

58   al., 2014; Perry and Lefticariu, 2014) or progressive alteration of marine minerals in meteoric

59   waters as they age (Levin et al., 2014; Perry and Lefticariu, 2014). This lack of uniqueness has

60   persisted since the first oxygen-isotope measurements of Archean cherts were reported over 50

61   years ago (Perry, 1967) because $\delta'^{18}O$ values alone cannot distinguish between changes in the

62   isotopic composition of the source water and changes in growth temperature. Clumped-isotope

63   approaches have emerged as a tool to constrain these quantities independently, but their

64   compositions in Precambrian carbonates have likely been altered by heating associated with burial

65   and exhumation (Henkes et al., 2018; Passey and Henkes, 2012; Stolper and Eiler, 2015). Other

66   approaches have been developed, such as $\delta'^{18}O$ values in occluded kerogen (Tartèse et al., 2017),

67   but the degree and nature of alteration in these archives is poorly known. Thus, the idea of a long-

68   term evolution in seawater $\delta'^{18}O$ values remains controversial.

69   We hypothesize that $^{18}O/^{16}O$ and $^{17}O/^{16}O$ isotope ratios of cherts—i.e., their triple oxygen-

70   isotope composition—can constrain the $\delta'^{18}O$ of ancient porewaters. Ultra-high-precision oxygen

71   triple-isotope measurements (quantified as $\Delta'^{17}O = \delta'^{17}O - 0.5305 \times \delta'^{18}O$) allow one to probe the

72    $\delta'^{18}O$-$\Delta'^{17}O$ relationships between phases, which are bounded by physical-chemical constraints

73   (Cao and Liu, 2011; Hayles et al., 2018; Hayles et al., 2017). For a given source-water $\delta'^{18}O$ and

74    $\Delta'^{17}O$ value, only a bounded range of chert compositions are possible at equilibrium (Hayles et al.,

75   2018; Sharp et al., 2016; Wostbrock et al., 2018). Similarly, the oxygen triple-isotope composition

76   of a given chert is only consistent with a narrow set of growth waters. The low permeability and

77   low oxygen diffusivity in microquartz cherts render them an ideal phase to analyze these variations

78   because they are resistant to alteration once the crystalline quartz phase has formed (Knauth,

79   1994): experimental measurements of oxygen diffusion rates in grain boundaries of natural chert

80   samples suggest it would take 30-300 Gyr for exchange to occur across a one-centimeter-thick

81   layer at 450°C (Farver and Yund, 1991).

82   Earth-system evolution models that predict lower seawater $\delta'^{18}O$ values early in Earth's

83   history require a lower ratio of high-temperature to low-temperature water-rock interactions in

84   Earth's deep past (Jaffrés et al., 2007; Kasting et al., 2006; Wallmann, 2004). An empirically

85   constrained model for seawater $\Delta'^{17}O$, based on the long-term water-rock mass balance formalism

86   of Muehlenbachs (1998), predicts higher seawater $\Delta'^{17}O$ values when $\delta'^{18}O$ values are low (Pack

87   and Herwartz, 2014; Sengupta and Pack, 2018).

88   To date, triple-oxygen compositions of only one set of Precambrian (2.5 Ga) and

89   Phanerozoic cherts has been published (Levin et al., 2014). Their compositions show no coherent

90   pattern, but are generally lower in $\Delta'^{17}O$ than expected for equilibrium with seawater at a given

91    $\delta'^{18}O$ value. Closed-system hydrothermal alteration was suggested as a potential driver of triple-

92   oxygen variability in the rock record, although one Phanerozoic chert (~65 Ma Stevns Klint chert)

93   was found to be unaltered (Sengupta and Pack, 2018). Given the sparsity of chert triple-oxygen

94   data, it is not known if the secular evolution in $\delta'^{18}O$ values is also present in $\Delta'^{17}O$ values. If the

95   secular evolution in chert $\delta'^{18}O$ values is mirrored in their $\Delta'^{17}O$ values, chert oxygen-isotope

96   compositions may be diagnostic of changing Earth-system processes through Earth history.

97   In this study, we expanded the record of triple-oxygen isotopes in chert by analyzing the

98   compositions of suite of marine cherts from the Archaean to late Phanerozoic. Higher $\Delta'^{17}O$ values

99   in ancient cherts, together with oxygen triple-isotope compositions that are incompatible with

100   growth in a modern ice-free ocean, would imply that the $\delta'^{18}O$ value of diagenetic fluids—and

101   perhaps seawater—has evolved over Earth history. Chert compositions compatible with growth in

102   modern-like diagenetic fluids (i.e. seawater) through Earth history would imply robust proportions

103 of global seawater-rock interactions and relatively constant diagenetic environments for marine

104 chert formation amidst a cooling lithosphere and evolving tectonic boundary conditions.

105 **2. Materials and Methods:**

106

107 **2.1 Materials**

108

109   Chert samples for this study were taken from units covering 3.4 billion years of Earth's

110 history from three modern day continents. Samples for this study were taken from the

111 Monterrey/Sisquoc Formation (Miocene) of California, San Andres Limestone (Permian) and

112 Onate formation (Devonian) of New Mexico, Caballos Novaculite (Devonian) and Ellenberger

113 Group (Ordovician) of Texas, Liuchapo Formation (Ediacaran) of China, Gunflint Formation

114 (1.880 Ga) in Ontario and the Frisco Formation (2.521 Ga), Moodies Group (3.22 Ga), Mendon

115 Formation (3.258 Ga) and Kromberg Formation (3.41 Ga) of South Africa. Specific localities,

116 references for the samples, GPS coordinates, where known, and some further sample information

117 can be found in Table S1 in the supplemental. Samples are selected based on purity because the

118 analytical technique for oxygen isotopes cannot discriminate between the silica component of

119 chert and detrital components. All samples have been analyzed by LA-ICPMS to verify purity is

120 greater than 98% SiO_2, but the results for only a subset of these samples are presented in the

121 supplemental with the remainder to be presented at a later date.

122

123

124 **2.2 Methods**

125   Oxygen isotope analyses were conducted at Rice University using techniques previously

126   described (Yeung et al., 2018). Prior to oxygen isotope analysis, 2-3 mg chert samples and

127   silicate standards are loaded onto a sample plate made of 316L steel. The sample plate is then

128   placed into a cell in the laser fluorination line equipped with a ThF_4 coated ZnSe window. The

129   cell is evacuated to high vacuum using a turbo pump and an infrared lamp is used to heat the

130   sample plate through the window. The heating and pumping are continued until the pressure

131   measured at the pump reads $<10^{-6}$ mbar. When all samples are individual grains, this heating step

132   typically lasts for 3 days, but can take up to a week if hydrous (e.g. opal) or powdered samples

133   are loaded. At the end of this step, the cell containing the samples is filled with ~30mbar of pure

134   F_2 gas generated by heating of a potassium fluoronickelate salt (Asprey, 1976). The purity of the

135   F_2 gas, and in particular the lack of O_2, is verified using periodic F_2-only blank tests mimicking

136   the fluorination procedure but lacking the laser heating step. The samples and standards are

137   exposed to the fluorine gas atmosphere at room temperature for two days. This prefluorination

138   step is done to remove any further traces of moisture from the samples but in no instance was an

139   O_2 yield from this step observed.

140   Oxygen from silica samples and silicate standards are converted to O_2 gas by reaction with

141   a two-fold excess of purified F_2 gas. Typical operating pressure of F_2 is 60 mbar. Heat for the

142   reaction is provided by a 10.6 μm CO_2 laser (Synrad 48-2; 25W). Reaction temperatures are

143   unknown, but the majority of the reaction proceeds above the melting temperature of the silicates

144   and yields are complete. For all chert samples, no residues remained in the cell after fluorination

145   indicating the samples were composed of pure silica as most common metal fluorides are solids

146   under the reaction conditions. The purity of the silica was confirmed for the samples which LA-

147   ICPMS and electron microprobe analyses were performed (see Supplemental Information). The

148   resulting gas mixture of F_2, O_2, SiF_4 and trace impurities (e.g. CF_4, NF_3) is first purified

149   cryogenically at -196°C to remove SiF_4 and any other condensable reaction products (e.g. trace

150   CF_4). This is followed by reaction of the F_2 with KBr held at 215°C and condensation of the

151   products at -196°C. The resulting roughly purified O_2 is collected onto a U-trap filled with silica

152   gel and forwarded through a 3.05 m × 1/8" OD gas chromatography (GC) column filled with

153   molecular sieve 5A (80/100 mesh) in a 20 mL/min flow of He carrier gas to remove any trace

154   NF_3. Beginning at ~2 minutes after introduction and ending 10 minutes after introduction, the

155   purified O_2 is recollected in a second silica gel filled U-trap. All processes after the fluorination

156   reaction are automated in order to reduce user-derived variability therein.

157   The resulting purified O_2 is analyzed for triple oxygen isotope composition on a Nu

158   Instruments *Perspective IS* mass spectrometer (PS001) equipped with a dual inlet and directly

159   connected to the fluorination line. Oxygen gas is transferred to the mass spectrometer through a 2

160   ml silica gel filled transfer tube equipped with an automated LN_2 pump. After collection, the O_2

161   is expanded into the sample bellow while the silica gel is heated to 95°C and the bellow is cycled

162   from 90% to 25% six times over 30 minutes. Similar to the fluorination line operation, sample

163   transfer to the mass spectrometer is automated to remove user dependencies. Machine analytical

164   precision for all delta values are 0.002‰ or less. Precision (1σ) for analysis of silica is 0.08‰ for

165    $\delta'^{18}O$ and 0.004‰ for $\Delta'^{17}O$ based on pooled variance of repeat analyses for silica samples

166   analyzed to date. Equivalent precisions are attained for UWG-2 (n=7) which is used as a pinning

167   standard (Valley et al., 1995).

168   Air O_2, used as a secondary standard for scaling purposes, is purified on a separate GC

169   column filled with molecular sieve 5A held at -80°C (3.05 m × 1/8" OD; Agilent 7890B GC with

170   thermal conductivity detector). The outflow of the GC separation is interfaced with the last

171   collection trap of the fluorination line allowing for sample transfer from the fluorination line to

172   be identical to that for O_2 from silicates.

173   The scale compression correction follows the 'traditional linear' scheme of Schoenemann et

174   al. (2013). Previously, we identified a scale compression in the raw isotope-ratio values from the

175   mass spectrometer which is significant for triple oxygen isotope measurements and can be

176   explained fully by a "pressure baseline" (PBL) effect (Yeung et al., 2018). The PBL effect

177   results from scattering of ions/electrons within the flight tube of the mass spectrometer and is

178   manifest as a nonzero baseline when the gas is entering the source. Provided that the beam

179   intensity is fixed based on the major beam (m/z=32), the selected scheme approximates the

180   theoretical correction of the PBL effect to well within analytical uncertainty (Yeung et al., 2018).

181

182

183   To compare our results directly with the temperature-dependent SiO_2-water fractionation

184   calibration of Sharp et al. (2016), we normalize isotope ratios against the UWG-2 standard, which

185   we assign a $\Delta'^{17}O$ value of -0.067‰ and a $\delta^{18}O$ value of 5.99‰ (Pack and Herwartz, 2014; Sharp

186   et al., 2016). The measured $\Delta'^{17}O$ values for UWG-2 and San Carlos Olivine (SCO) differ by ~10

187   ppm on our setup. This result disagrees with that of (Pack and Herwartz, 2014), which showed

188   only a 1 ppm difference between these standards. Considering that our SCO sample (SCO99-olv)

189   may differ from that of other laboratories and that our measured compositions of SCO yield more

190   variability than our measurements of UWG-2, we use UWG-2 as the primary standard. Further

191   scaling of the triple-oxygen results is done by assigning a fixed difference in oxygen isotope

192   compositions between Air-O_2 and UWG-2. The values used are $\Delta(\delta^{18}O)_{Air - UWG-2} = 17.4‰$,

193   consistent with PBL corrected measurements from our laboratory and $\Delta(\Delta'^{17}O)_{Air - UWG-2} = $ -

194   0.421‰ which is consistent with previously published values corrected to VSMOW2-SLAP

195   scaling (Yeung et al., 2018). This scheme yields inter-laboratory agreement in standard materials

196   within 10 ppm for $\Delta'^{17}O$ (Yeung et al., 2018).

197
198   **3. Results:**
199
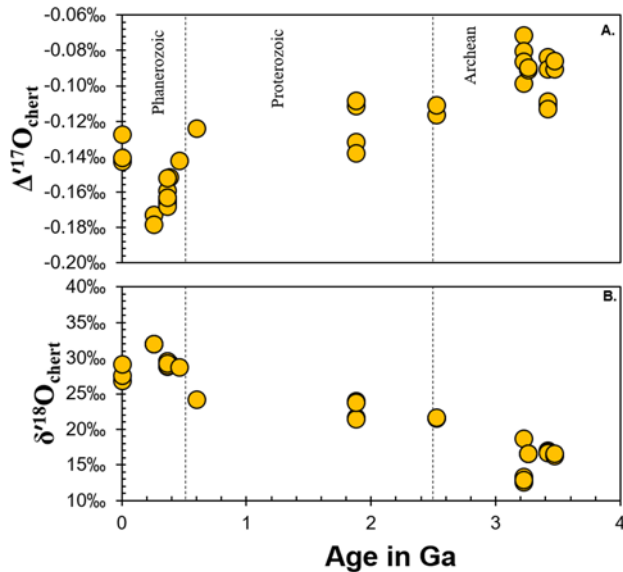
200
201   *Fig. 1. Oxygen triple-isotope composition of cherts through time. **a.** Measured $\Delta'^{17}O$ of cherts*
202   *analyzed for this study. Point size is plotted to the precision of the measurement (0.004‰ 1σ). **b.***
203   *Measured $\delta'^{18}O(=ln[\delta^{18}O+1])$ of cherts analyzed for this study. Uncertainties for $\delta'^{18}O$ (0.08‰)*
204   *are smaller than the point size.*

205
206
207   The cherts show a trend of increasing $\delta'^{18}O$ and decreasing $\Delta'^{17}O$ values through time

208   (Fig.1). The total range in $\Delta'^{17}O$ values is approximately 0.1‰, with an average decrease of

209   0.02‰ per billion years. Phanerozoic marine cherts are characterized by $\lambda = 0.5223 \pm 0.0014$

210   (1σ; the slope of a $\delta'^{17}O$ vs. $\delta'^{18}O$ cross-plot), and Precambrian cherts by $\lambda = 0.5263 \pm 0.0006$.

211   These λ values suggest that different processes and/or reservoirs govern oxygen triple-isotope

212   variations in Phanerozoic and Precambrian cherts. Where repeat analyses were done (majority of

213   samples; see supplemental) different analyses of the same band or region of the cherts yields

214   nearly equivalent results, indicating homogeneity of oxygen isotopes in these samples at spatial

10

215   scales greater than our sampling scale (~1 mm^3). Our choice to use the pooled variance of these

216   analyses for our analytical uncertainty means that any homogeneity at this scale is factored into

217   our uncertainty (±0.004‰ for $\Delta'^{17}O$ and ±0.08‰ for $\delta'^{18}O$).

218

219   **4. Discussion**

220

221   **4.1 Phanerozoic cherts**
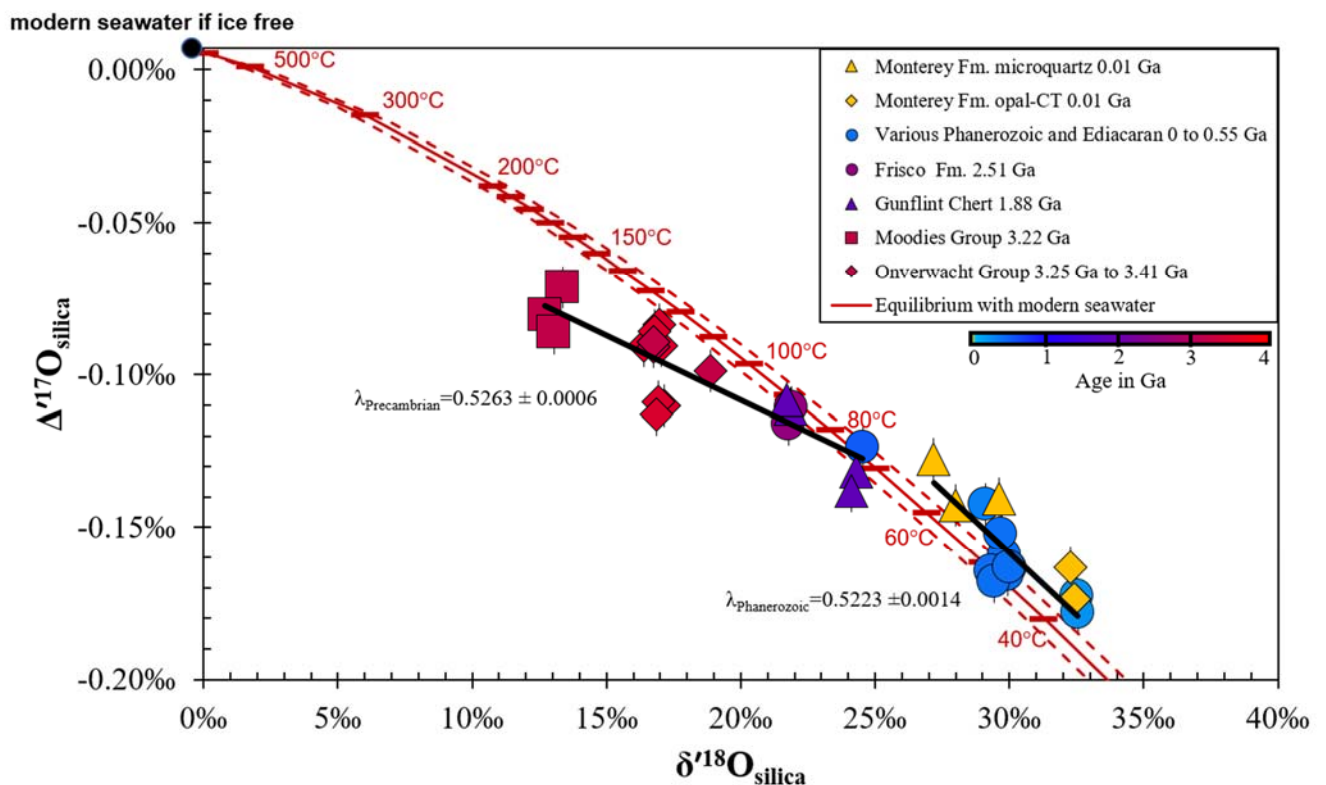

Fig. 2. $\delta'^{18}O$ vs. $\Delta'^{17}O$ of cherts and two Neogene Opal-CT samples. Uncertainties are the same as in Fig. 1. The red curve is the range of silica triple-oxygen isotope compositions compatible with formation in the modern ice-free ocean [$\delta^{18}O$= -1‰, $\Delta'^{17}O$ = 0.0075‰ calculated using data in Sharp et al. (2018)] based on the empirical silica-water fractionation estimate of Sharp et al.(Sharp et al., 2016) with slight modification from Wostbrock et al. (2018). Dotted lines around the fractionation curve correspond to compositions of water ±1‰ from a modern ice-free ocean.

222   The oxygen-isotope compositions of chert and opal-CT in the Miocene Monterey

223   Formation (0.01 Ga) are consistent with growth from a water that has a composition offset from

224   a modern (ice-free) ocean by either +1.5‰ in $\delta^{18}O$, +0.008‰ in $\Delta'^{17}O$, or some intermediate

225   composition within those bounds (see Fig. 2). This difference could be explained by slight

226   analytical differences between our calibration and that used for the silica-water fractionation

227   curve (Sharp et al., 2016; Wostbrock et al., 2018). Therefore, the growth waters for these cherts

228   are isotopically indistinguishable from ice-free modern seawater (hereafter "isotopically

229   modern" seawater), although a small porewater oxygen-isotope change during chert diagenesis

230   cannot be ruled out. The Miocene opal and chert compositions are plausibly explained by an

231   open seawater-porewater system that recrystallizes silica at various temperatures during burial.

232   This interpretation is consistent with previous work on silica (Murata et al., 1977) and carbonates

233   (Loyd et al., 2012) in diagenetic settings that showed little evidence for significant porewater

234    $\delta^{18}O$ evolution. We thus interpret the λ value of 0.5223 from the Miocene cherts to result from

235   chert recrystallization in pore waters of constant isotopic composition over a range of

236   temperatures. For this environment, the diagenetic fluid appears to be a proxy for the isotopic

237   composition of coeval seawater.

238   Similar to the Miocene cherts, the oxygen-isotope compositions of older Phanerozoic

239   cherts are consistent with growth from a fluid resembling modern seawater in its oxygen-isotope

240   composition. Implied growth temperatures based on $\delta'^{18}O$ in such waters are between

241   approximately 35°C and 60°C, with a modal temperature of 47°C and no clear correlation

242   between temperature and age. These conditions, and the range in $\delta'^{18}O$ and $\Delta'^{17}O$ values, are

243   consistent with early diagenetic transformation of low-detritus Opal-A to Opal-CT or

244   microquartz beneath the seafloor (Keller and Isaacs, 1985). Furthermore, samples identified as

245   opal-CT from the Monterey Formation (Table S3) yield formation temperatures near 35°C,

246   which are consistent with the expectation of lower diagenetic temperatures associated with opal-

247   CT formation (Keller and Isaacs, 1985). This result suggests (1) the isotopic equivalence of

248   seawater and pore fluids in the environment of chert diagenesis holds through the Phanerozoic

249   and (2) the oxygen isotope composition of seawater has remained roughly constant since at least

250   the Ordovician. This latter interpretation corroborates recent carbonate clumped-isotope results,

251   which suggest a seawater $\delta^{18}O$ value bound within ~2‰ since the Cambrian (Coogan et al.,

252   2019; Cummins et al., 2014; Henkes et al., 2018; Ryb and Eiler, 2018).

253   Previously Phanerozoic and Archean cherts were measured by Levin et al. (2014) who

254   reported $\Delta'^{17}O$ values relative to UWG-2 measured in their laboratory. Normalizing their chert

255   results to the UWG-2 composition used here yields mean $\Delta'^{17}O$ values that are lower than ours

256   by 0.1‰. The reason for this difference cannot be determined with the information provided in

257   Levin et al. (2014), although the larger uncertainties in $\Delta'^{17}O$ standards (e.g., $1\sigma = 0.052$‰ for

258   UWG-2 and 0.035‰ for NBS-28) suggest that at least some part of the disagreement can be

259   explained by random error. Potential unquantified triple-oxygen scale compression is difficult to

260   diagnose in that study given the small $\delta'^{18}O$ range (4‰) of the standards used. We note that our

261   reported Phanerozoic chert compositions more closely match marine quartz compositions with

262   approximately the same $\delta^{18}O$ reported in Sharp et al. (2018).

263

264   **4.2 Precambrian Cherts**

265   Unlike for the Phanerozoic cherts, the oxygen-isotope compositions of the Latest

266   Archean and Proterozoic cherts require diagenetic recrystallization at higher temperatures (70-

267   90°C) and/or in isotopically different waters from those of the Phanerozoic. Paleoarchean cherts

268   cannot have formed in isotopically modern seawater, invalidating an early hypothesis that they

269   had grown at elevated temperatures from such fluids (Knauth and Lowe, 2003). Potential

270   explanations for triple-oxygen compositions of Precambrian cherts involve scenarios in which (*i*)

271   the initial growth fluids had a different isotopic composition, (*ii*) the cherts are internally mixed,

272   i.e., representing multiple generations of silica precipitation that occurred under different

273   conditions, or (*iii*) the cherts have been altered after initial deposition. Below, we evaluate these

274   potential explanations for the isotopic composition of Precambrian cherts, with a focus on those

275   of the Paleoarchean.

276

4.2.1 Scenarios 1 and 2: Early diagenesis in low-$\delta'^{18}O$, high-$\Delta'^{17}O$ fluids

278   If the early diagenesis of Phanerozoic cherts is a satisfactory model, i.e., recrystallization

279   occurred between 35°C and 60°C, then one can estimate the fluid composition required to

280   precipitate Precambrian cherts in that environment. Using this approach, the oxygen triple-

281   isotope composition of Onverwacht Group cherts ($\delta'^{18}O$ = 17.165‰, $\Delta'^{17}O$ = -0.090‰ on

282   average) imply a diagenetic fluid of $\delta'^{18}O$ = ⁻16.4‰ to ⁻10.7‰ and $\Delta'^{17}O$ = 0.103‰ to 0.057‰

283   for the Paleoarchaean. Under this interpretation, younger cherts are compatible with growth in

284   fluids that were isotopically closer to modern seawater, but those fluids still must have lower

285    $\delta'^{18}O$ and higher $\Delta'^{17}O$ values. The origins of these low-$\delta'^{18}O$, high-$\Delta'^{17}O$ fluids is enigmatic; we

286   explore the possibility that lighter diagenetic fluids represent (1) meteoric waters and (2) coeval

287   seawater.

288   The Precambrian cherts can be described by a singular trend different from the

289   Phanerozoic cherts, with a λ value of 0.5263. This λ value is indistinguishable from that

290   characterizing meteoric waters with $\delta^{18}O$ > -20‰ [λ = 0.5265 ± 0.0003; (Sharp et al., 2018)]. A

291   possible explanation for the compositions of Precambrian cherts is thus subsurface intrusion of

292   meteoric waters into the early diagenetic environment where they recrystallized. The isotopically

293   lightest cherts presented here would require nearly pure meteoric waters with low $\delta'^{18}O$ values $\leq$

294   -11‰ if water-to-rock ratios are high. Explaining the temporal trend in triple-oxygen

295   composition using this mechanism requires that meteoric water be a ubiquitous component of

296   Precambrian chert growth fluids, but insignificant for their Phanerozoic equivalents. If this

297   interpretation is correct, then the need for this dichotomy in chert formation conditions is further

298   evidenced by larger compilations of chert $^{18}O/^{16}O$ ratios (Bindeman et al., 2016). Whether a

299   secular change in chert diagenesis of this nature occurred over Earth history is not known.

300   However, it is clear from studies of the Paleoarchean cherts of the Onverwacht Group

301   (3.41 Ga to 3.25 Ga; plotted as diamonds in Figure 2) and the Buck Reef chert in particular

302   (BRC; 3.41 Ga), that at least some Paleoarchean cherts underwent early diagenetic

303   recrystallization in an environment similar to that for the Phanerozoic cherts (Knauth and Lowe,

304   2003). The lines of supporting evidence include: the range of $\delta'^{18}O$ values matching the ~7‰

305   range of Phanerozoic cherts (despite lower mean values), the apparent early silicification and

306   brecciation of "white cherts" of the BRC and Mendon Formation, and silicification prior to the

307   compaction of carbonaceous particles and relicts of opal-CT lepispheres (Hren et al., 2009;

308   Knauth and Lowe, 2003; Stefurak et al., 2015; Tice and Lowe, 2006; Trower and Lowe, 2016).

309   Furthermore, the chert shows no evidence for exogenous inputs from meteoric waters based on

310   δD-$\delta^{18}O$ trends, which are more consistent with early diagenesis at temperatures below 55°C

311   (Hren et al., 2009). The recrystallization fluid for the samples in that study were thus interpreted

312   to be coeval diagenetic fluids.

313   The samples of BRC analyzed this study were sampled from one of two sections utilized

314   in the Hren et al. (2009) study, so their geologic context is presumed to apply. If the composition

315   of the BRC "white" chert is used to solve for the porewater composition—because they are of

316 higher purity (Table S2), show no textural evidence of secondary silica (Figure S4), and are

317 believed to have silicified first—then the diagenetic fluid would have $\delta'^{18}O = -16.6‰$ to $-11.0‰$

318 and $\Delta'^{17}O = 0.092‰$ to $0.044‰$, still different from isotopically modern seawater. Note that the

319 white chert from the BRC analyzed here has a lower $\delta'^{18}O$ (16.9‰) than equivalent samples

320 from the previous study, with a composition closer to the black cherts in the unit. It may indicate

321 that these particular samples of white chert recrystallized at roughly the same temperature as the

322 surrounding black chert. In general, the measured cherts from this age have $\delta'^{18}O$ values at the

323 low end of those previously measured (Hren et al., 2009; Knauth and Lowe, 2003). Cherts with

324 these compositions have been previously interpreted as representing the highest-temperature

325 diagenetic phase.

326 Interestingly, the two 1.88 Ga Gunflint cherts measured here define a triple-oxygen trend

327 roughly parallel to the trend observed for the Phanerozoic cherts. This parallel trend may imply a

328 similar diagenetic environment in a fluid of intermediate composition (i.e., $\delta^{18}O \sim -4‰$), but

329 with the limited data currently available it is not yet possible to determine if this trend is

330 coincidental. Parallel, triple-isotope trends resembling the Phanerozoic trend within a sequence

331 would be evidence that the chert oxygen-isotope compositions reflect an early diagenetic

332 environment similar to Phanerozoic cherts.

333

334

4.2.2 Scenario 3: Mixtures of high- and low-temperature phases
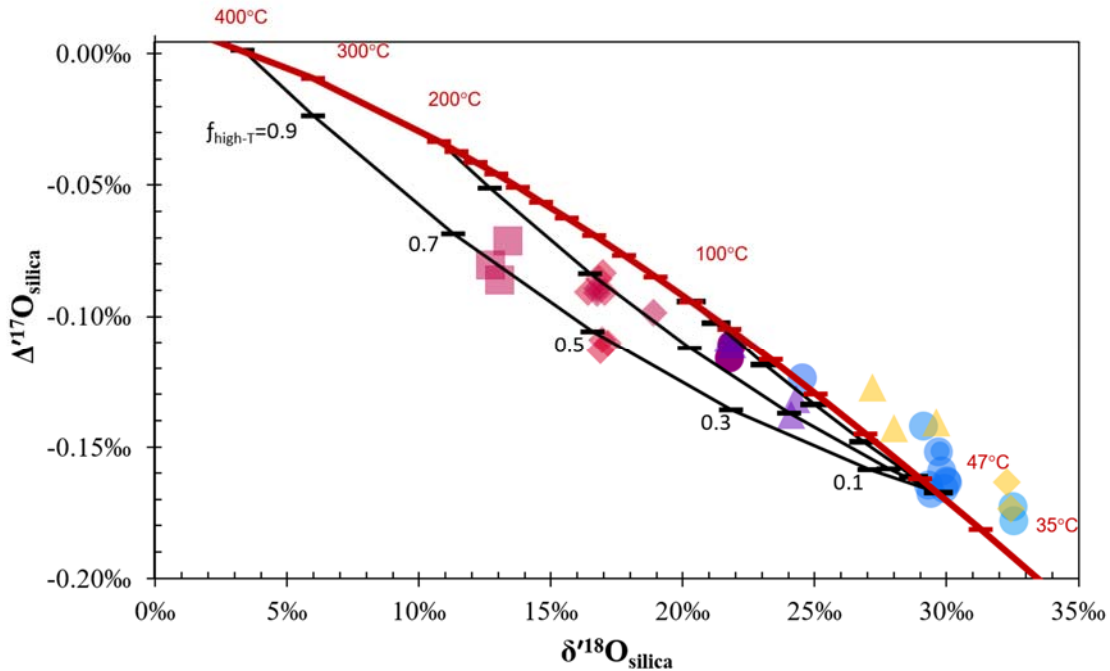
Fig. 3. High and low temperature chert mixture models. The red curve is the range of silica triple-oxygen isotope compositions compatible with formation in modern ice-free seawater). Black lines are two-endmember mixing curves between a higher temperature chert endmember and a lower temperature endmember that were crystallized in porewaters of the same isotope composition. The chert triple oxygen isotope compositions are plotted for comparison.

An alternative explanation for the triple-isotope compositions of Precambrian cherts is for them to be mixtures of silica crystallized at different temperatures. Figure 3 shows two-endmember mixing curves for high- and low-temperature silica mixtures assuming the pore water composition in the two environments is equal to isotopically modern seawater. All the Precambrian cherts can be explained as mixtures of silica crystallized in early diagenetic environments and silica

349   crystallized between 100˚C and 400˚C. Generally, the Archaean cherts require a higher-

350   temperature silica mixing endmember than the Proterozoic cherts. The secular trend in oxygen-

351   isotope compositions would then reflect a cooling of the high-temperature endmember over Earth

352   history.

353   If the cherts analyzed here are mixtures of high- and low-temperature silica, the

354   heterogeneity would need to manifest at a scale <1 mm^3, perhaps at the scale of microquartz grains

355   (10^{-5} mm^3). Microanalytical techniques may be able to test this hypothesis. A broad distribution in

356   δ^{18}O has been observed in some Precambrian cherts, particularly those of the 1.88 Ga Gunflint

357   Formation, examples of which were also analyzed here (triangles in Figures 2 and 3). Previous

358   work indicated an isotopic heterogeneity of ~12‰ at a 2 μm scale in the Gunflint chert, which was

359   taken as evidence for the presence of a ~130°C hydrothermal silica mixing endmember (Marin et

360   al., 2010). Mixing between a high-temperature silica endmember at 120°C (~40%) and a low-

361   temperature silica endmember at 47˚C (~60%), both formed in isotopically modern seawater, can

362   explain the triple-oxygen composition of our Gunflint chert samples. However, this particular

363   mixture is not unique; there exists a continuum of scenarios for two-endmember (high- and low-

364   temperature silica) mixtures that can explain these samples if the oxygen-isotope composition of

365   the growth fluid is allowed to vary. For example, a difference in δ^{18}O of 12‰ can also be attained

366   if the two end members formed in the same water at temperatures of ~20°C and ~70°C, as is

367   reasonable for the early diagenetic environment. This particular scenario is compatible with water

368   compositions of δ^{18}O < -4‰ using the bulk oxygen isotope compositions of Gunflint chert

369   measured here.

370

371

372   **4.2.3 Scenario 4: Late, closed-system recrystallization of silica**

373

374   Finally, we investigate closed-system recrystallization as a possible explanation for the

375   oxygen-isotope trends in Precambrian cherts. This mechanism was previously considered by

376   Sengupta and Pack (2018), although our formulation differs slightly in implementation. The

377   equations for the closed-system water-rock interactions are given by:

378

379

380     $$\left(\frac{W}{R}\right) R_{w,i} + R_{r,i} = R_{w,f}\left[\alpha + \left(\frac{W}{R}\right)\right] \qquad\qquad \text{Eq.1}$$

381

382   where R is the ratio of the heavy isotope to the light isotope, i.e., $^{17}O/^{16}O$ or $^{18}O/^{16}O$, α is the

383   temperature dependent fractionation factor for the rock (SiO_2) relative to water, the subscripts w

384   and r indicate the parameters for water and rock, respectively, and the subscripts i and f indicate

385   initial and final compositions, respectively. W and R are the amounts of oxygen held in water and

386   the silica phase, respectively.

387
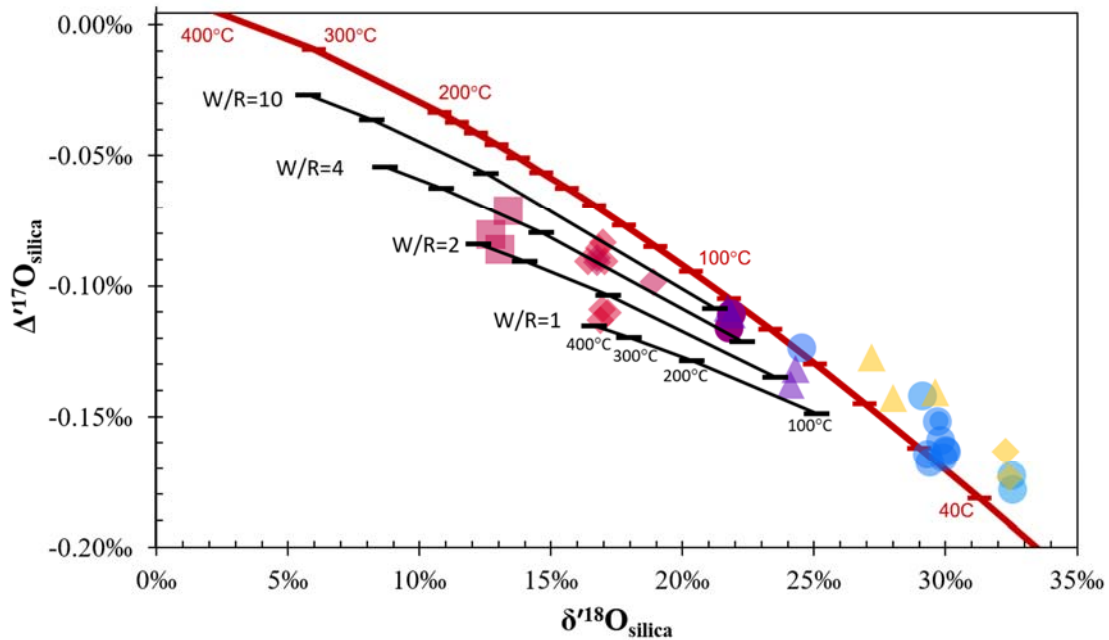
Fig. 4. *Closed-system chert recrystallization model results. The red curve is the range of silica triple-oxygen isotope compositions compatible with formation in modern ice-free seawater. Black lines give results for closed-system recrystallization at a range of water-rock ratios (W/R) and temperatures. The chert triple oxygen isotope compositions are plotted for comparison.*

393

We find that for cherts initially formed at 47˚C (in modern seawater) and diagenetic fluids resembling modern seawater, the secular trend of Precambrian cherts can be explained by closed-system recrystallization for $1 \leq W/R \leq 10$ (see Fig. 4); however, the temperature of alteration must undergo a secular decrease through Earth' history. For example, using $W/R = 4$, the Onverwacht cherts (~3.4 Ga) would be best explained with a closed-system alteration temperature of 175°C, while the cherts from the Frisco Formation (2.51 Ga) require a temperature of 110°C. If the

400   diagenetic fluid were meteoric instead, higher water-to-rock ratios are needed to explain the chert

401   compositions, but secular cooling of those fluids is still required.

402   The need for high water-to-rock ratios argues against the water-rock system being closed

403   at the grain-scale; for example, if the initial phase consisted of silica granules, as might be implied

404   by the presence of ripples and cross bedding in the Onverwacht cherts (Tice and Lowe, 2006), then

405   using a typical porosity of 35%, the bulk W/R ratio is calculated to be ~0.34. Instead, higher water-

406   to-rock ratios require that the closed system is at the formation scale, perhaps consisting of a

407   permeable, but unreactive rock that is spatially separated from the samples being analyzed. To

408   achieve a W/R ratio of 1 using a nominal water-filled porosity of 0.35 would require that 66% of

409   the rock in the system is unreactive. Higher water-to-rock ratios would require more of the system

410   to be unreactive, for instance 91% unreactive to reach a W/R of 4. Such a scenario could result

411   from exchange occurring fastest at the base of a sediment column, where temperatures are highest,

412   but at a rate slower than the circulation rate of the fluid within the system. In that case, one might

413   expect distinct closed-system recrystallization trends down-section for different formations in

414   which permeabilities, porosities, burial rates, and thermal histories differ. In effect, the diagenetic

415   fluids of these formations would all be different, yielding disparate trajectories in triple-isotope

416   space. More exhaustive compilations of chert triple-isotope data, once available, will be able to

417   test this hypothesis.

418

419

420   **4.3. Potential implications and relationship to other proxies for ancient temperatures**

421   We will first explore the implications if the BRC samples crystallized in Paleoarchaean

422   diagenetic fluids. Here, we use the interpretation that the BRC represents a diagenetic sequence

423   similar to that of Phanerozoic cherts (Hren et al., 2009; Knauth and Lowe, 2003). $\delta'^{18}O$ values as

424   high as 22‰ have been reported in the BRC and interpreted to reflect the lowest-temperature

425   diagenetic phase in the unit (Knauth and Lowe, 2003). Thus, using $\delta'^{18}O = ^-11$‰ for the diagenetic

426   fluid and $\delta'^{18}O = 22$‰ for the BRC yields a minimum diagenetic temperature of 37°C. This

427   temperature also serves as an upper limit on seafloor temperatures for this locality during the

428   Paleoarchean. The relatively low temperature is in agreement with the temperature limit (<55°C)

429   inferred from δD-$\delta'^{18}O$ pairings (Hren et al., 2009) and the presence of possible diamictites and

430   gypsum pseudomorphs in lower units of the Onverwacht (de Wit and Furnes, 2016). Moreover, it

431   is feasible based on recent climate-model predictions (Charnay et al., 2017; Krissansen-Totton et

432   al., 2018) We note that a minimum diagenetic temperature of 37°C aligns with the lowest

433   temperature of chert diagenesis we observe in Phanerozoic cherts (~35°C), making this estimate

434   and interpretation self-consistent.

435

436   The cherts of the Onverwacht Group have been interpreted as marine due to the large lateral

437   extent of the chert units, the need for large amounts of silica to account for hundreds of meters of

438   silicified rocks and the presence of evaporites (indicating a saline environment). Thus, interpreting

439   the chert growth waters as the coeval diagenetic fluid leads naturally to the interpretation that

440   seawater in the Archean was significantly isotopically lighter. If the diagenetic fluid approximates

441   coeval seawater for the Precambrian samples—as is case for Phanerozoic cherts—the triple-

442   isotope data suggest that seawater became progressively more ^{18}O-enriched over geologic time

443   (Fig. S1). Any feasible mechanisms for accomplishing a lower $\delta'^{18}O$ for Paleoarchean seawater

444   require more intense low temperature water-rock interactions and/or less intense high temperature

445   water-rock interactions earlier in Earth's history (Jaffrés et al., 2007; Kasting et al., 2006; Pack

446 and Herwartz, 2014; Wallmann, 2004). Modeling studies suggest that a seawater $\delta'^{18}O$ value of -

447 11‰ can only be achieved by dramatically reducing the proportion of water-rock interactions

448 occurring at high temperatures (Jaffrés et al., 2007; Kasting et al., 2006). Such a scenario could be

449 realized if submarine magmatic centers were shallower in the Archean, perhaps associated with

450 higher mid-ocean ridge crests or more extensive volcanic plateaus (Kamber, 2010; Kasting et al.,

451 2006; Lambert, 1980). Alternatively, a more sluggish tectonic regime in the Archean (Tang et al.,

452 2016), characterized by a reduced area of magmatic activity, could lead to a reduction in high-

453 temperature water-rock chemistry.

454   The Archaean seawater composition implied by the early-diagenesis interpretation of

455 Archean cherts can be compared with estimates obtained from other proxies. The $\delta'^{18}O$ values in

456 iron-associated phosphate and kerogen-bound oxygen (Blake et al., 2010; Tartèse et al., 2017) may

457 first appear to be in disagreement, but the reported uncertainties of those approaches allow them

458 to be compatible with local surface water having $\delta'^{18}O \geq {}^-10‰$ (Chang and Blake, 2015; Tartèse

459 et al., 2017). Thus, the composition of seawater is not further constrained by these proxies.

460   Sengupta and Pack (2018) recently constructed an empirically constrained seawater triple-

461 isotope model based on the model of Muehlenbachs (1998). The mass-balance model yields a λ

462 value for seawater evolution of 0.51, which is incompatible with the λ value of 0.526 from

463 Precambrian cherts in this study if they indeed formed in a fluid resembling Paleoarchaean

464 seawater. Reconciling the geological constraint indicating that the cherts of the Onverwacht Group

465 in general, and the BRC specifically, represent a diagenetic environment with this study requires

466 the diagenetic fluids be isotopically depleted relative to coeval seawater. Further constraints can

467 be provided with additional chert triple oxygen isotope compositions.

468   The other scenarios we consider, i.e. the involvement of meteoric water, late closed system

469   recrystallization and mixtures between silica formed at high temperature and low temperatures,

470   imply other secular Earth system trends. In the case of the involvement of meteoric water, a trend

471   in paleolatitude or paleoaltitude of the source waters would be needed to explain the chert

472   compositions. Another possible explanation is that of progressive alteration in meteoric waters

473   over the cherts long history, but this has been argued against in the past (Knauth and Lowe, 2003).

474   For the other potential explanations, the common trend is the need to invoke a secular change in

475   the temperature of later alteration. Assuming burial rates are constant, as they would be governed

476   by surface processes, the simplest explanation is a secular change in the geothermal gradient in the

477   environment of chert diagenesis. A steeper geothermal gradient in the Archean would bring the

478   depth with sufficient temperature closer to the surface possibly allowing these cherts to reach the

479   needed temperatures prior to the loss of their porosity. This may be explained by higher heat

480   production for the young Earth. Although studies estimating Archean geothermal gradients largely

481   focus on the gradient at greater depth, geothermal gradients on Archean cratons are thought to be

482   similar to the modern (Ballard and Pollack, 1988; Lenardic, 1998). It is unclear if near-surface

483   geothermal gradients should be sufficiently higher in Earth's deep past.

484   Regardless of the interpretation, the presence of a long-term triple-oxygen isotope trend in

485   Precambrian cherts implies a secular evolution of some boundary condition relevant to chert

486   diagenesis affecting the isotopic composition of the fluid. Moreover, this evolution appears to have

487   ceased by the beginning of the Phanerozoic, or has not yet significantly affected Phanerozoic

488   cherts. Examples of these boundary conditions are the composition of intruding meteoric waters

489   (e.g. driven by steadily decreasing paleolatitude for the sections), the global-mean temperature of

490   seawater-rock interactions (i.e. resulting in a change in seawater $\delta'^{18}O$) or the temperature of

491 hypothetical high-temperature alterations (i.e. secular change in the geotherm). These potential

492 explanations are not exclusive and any combination of them would be consistent with chert oxygen

493 isotope results. We note that shales, carbonates, and cherts share similar oxygen-isotope trends

494 through geologic time (Bindeman et al., 2016); our chert $\Delta'^{17}O$ record resembles that recently

495 reported for shale, in particular [(Bindeman et al., 2018); see also Fig. S1]. A parsimonious

496 explanation for the overall trend is the $\delta'^{18}O$ value of seawater evolved from -11‰ or lower during

497 the Paleoarchean to a modern composition by the Ordovician. However, conflicting geochemical

498 and modeling evidence in the literature precludes a definitive interpretation at this time (Blake et

499 al., 2010; Sengupta and Pack, 2018; Tartèse et al., 2017).

500

5.1 Conclusions:

502 The triple-oxygen isotope composition of marine cherts from 3.5 billion years of Earth's

503 history indicate a switch in some aspect of the factors leading to the oxygen isotope composition

504 of chert occurring at some time prior to the Ordovician. The oxygen isotope composition of

505 Phanerozoic cherts reflect recrystallization over a range of early diagenetic temperatures (35°C-

506 60°C) in a water indistinguishable from that of the modern ocean ($\delta^{18}O = 0 \pm 2$‰). Importantly,

507 the additional constraint provided by ^{17}O shows that low $\delta^{18}O$ values of Archean cherts are

508 incompatible with a hot (>70°C) surface and an isotopically modern oceans in the Archaean.

509 Geological and geochemical constraints from the literature implying an early diagenetic origin

510 for a subset of the measured Archean cherts, when combined with the data presented here,

511 suggests that at 3.45 Ga diagenetic fluids had a $\delta^{18}O$ value of < -11‰, with surface temperatures

512 <34°C. While this result may be used to indicate a secular evolution or seawater $\delta'^{18}O$, alternate

513 feasible explanations for the chert compositions remain which do not require a change in

514 seawater $\delta'^{18}O$.

515

521 **Author contributions:** The manuscript was written by Justin Hayles and Laurence Yeung. Field

522 work was conducted by Justin Hayles, Asmita Banerjee, Bing Shen and Martin Homann. Oxygen

523 isotope analysis was conducted by Justin Hayles. LA-ICPMS analysis was conducted by Justin

524 Hayles and Hehe Jiang. All authors contributed to interpretations.

525

References

Asprey, L.B., 1976. The Preparation of Very Pure Fluorine Gas. Journal of Fluorine Chemistry 7, 359-361.

Ballard, S., Pollack, H.N., 1988. Modern and ancient geotherms beneath southern Africa. Earth and Planetary Science Letters 88, 132-142.

Bindeman, I.N., Bekker, A., Zakharov, D.O., 2016. Oxygen isotope perspective on crustal evolution on early Earth: A record of Precambrian shales with emphasis on Paleoproterozoic glaciations and Great Oxygenation Event. Earth and Planetary Science Letters 437, 101-113.

Bindeman, I.N., Zakharov, D.O., Palandri, J., Greber, N.D., Dauphas, N., Retallack, G.J., Hofmann, A., Lackey, J.S., Bekker, A., 2018. Rapid emergence of subaerial landmasses and onset of a modern hydrologic cycle 2.5 billion years ago. Nature 557, 545-548.

Blake, R.E., Chang, S.J., Lepland, A., 2010. Phosphate oxygen isotopic evidence for a temperate and biologically active Archaean ocean. Nature 464, 1029.

Cao, X.B., Liu, Y., 2011. Equilibrium mass-dependent fractionation relationships for triple oxygen isotopes. Geochimica Et Cosmochimica Acta 75, 7435-7445.

Chang, S.J., Blake, R.E., 2015. Precise calibration of equilibrium oxygen isotope fractionations between dissolved phosphate and water from 3 to 37°C. Geochimica et Cosmochimica Acta 150, 314-329.

Charnay, B., Le Hir, G., Fluteau, F., Forget, F., Catling, D.C., 2017. A warm or a cold early Earth? New insights from a 3-D climate-carbon model. Earth and Planetary Science Letters 474, 97-109.

Coogan, L.A., Daëron, M., Gillis, K.M., 2019. Seafloor weathering and the oxygen isotope ratio in seawater: Insight from whole-rock $\delta 18O$ and carbonate $\delta 18O$ and $\Delta 47$ from the Troodos ophiolite. Earth and Planetary Science Letters 508, 41-50.

Cummins, R.C., Finnegan, S., Fike, D.A., Eiler, J.M., Fischer, W.W., 2014. Carbonate clumped isotope constraints on Silurian ocean temperature and seawater $\delta 18O$. Geochimica et Cosmochimica Acta 140, 241-258.

de Wit, M.J., Furnes, H., 2016. 3.5-Ga hydrothermal fields and diamictites in the Barberton Greenstone Belt—Paleoarchean crust in cold environments. Science Advances 2.

Farver, J.R., Yund, R.A., 1991. Measurement of oxygen grain boundary diffusion in natural, fine-grained, quartz aggregates. Geochimica et Cosmochimica Acta 55, 1597-1607.

Gregory, R.T., Taylor, H.P., 1981. An oxygen isotope profile in a section of Cretaceous oceanic crust, Samail Ophiolite, Oman: Evidence for $\delta 18O$ buffering of the oceans by deep (>5 km) seawater-hydrothermal circulation at mid-ocean ridges. Journal of Geophysical Research: Solid Earth 86, 2737-2755.

Hayles, J., Gao, C., Cao, X., Liu, Y., Bao, H., 2018. Theoretical calibration of the triple oxygen isotope thermometer. Geochimica et Cosmochimica Acta 235, 237-245.

Hayles, J.A., Cao, X., Bao, H., 2017. The statistical mechanical basis of the triple isotope fractionation relationship. Geochemical Perspectives Letters 3, 1-11.

Henkes, G.A., Passey, B.H., Grossman, E.L., Shenton, B.J., Yancey, T.E., Pérez-Huerta, A., 2018. Temperature evolution and the oxygen isotope composition of Phanerozoic oceans from carbonate clumped isotope thermometry. Earth and Planetary Science Letters 490, 40-50.

Hren, M.T., Tice, M.M., Chamberlain, C.P., 2009. Oxygen and hydrogen isotope evidence for a temperate climate 3.42 billion years ago. Nature 462, 205-208.

Jaffrés, J.B.D., Shields, G.A., Wallmann, K., 2007. The oxygen isotope evolution of seawater: A critical review of a long-standing controversy and an improved geological water cycle model for the past 3.4 billion years. Earth-Science Reviews 83, 83-122.

Kamber, B.S., 2010. Archean mafic-ultramafic volcanic landmasses and their effect on ocean atmosphere chemistry. Chem. Geol. 274, 19-28.

Kasting, J.F., Howard, M.T., Wallmann, K., Veizer, J., Shields, G., Jaffrés, J., 2006. Paleoclimates, ocean depth, and the oxygen isotopic composition of seawater. Earth and Planetary Science Letters 252, 82-93.

Keller, M.A., Isaacs, C.M., 1985. An evaluation of temperature scales for silica diagenesis in diatomaceous sequences including a new approach based on the Miocene Monterey Formation, California. Geo-Marine Letters 5, 31-35.

Knauth, L.P., 1994. Petrogenesis of chert. Reviews in Mineralogy and Geochemistry 29, 233-258.

Knauth, L.P., Epstein, S., 1976. Hydrogen and oxygen isotope ratios in nodular and bedded cherts. Geochimica et Cosmochimica Acta 40, 1095-1108.

Knauth, L.P., Lowe, D.R., 2003. High Archean climatic temperature inferred from oxygen isotope geochemistry of cherts in the 3.5 Ga Swaziland Supergroup, South Africa. Geological Society of America Bulletin 115, 566-580.

Krissansen-Totton, J., Arney, G.N., Catling, D.C., 2018. Constraining the climate and ocean pH of the early Earth with a geological carbon cycle model. Proceedings of the National Academy of Sciences.

Lambert, R.S.J., 1980. The thermal history of the earth in the Archean. Precambrian Research 11, 199-213.

Lenardic, A., 1998. On the partitioning of mantle heat loss below oceans and continents over time and its relationship to the Archaean paradox. Geophysical Journal International 134, 706-720.

Levin, N.E., Raub, T.D., Dauphas, N., Eiler, J.M., 2014. Triple oxygen isotope variations in sedimentary rocks. Geochimica Et Cosmochimica Acta 139, 173-189.

Loyd, S.J., Corsetti, F.A., Eiler, J.M., Tripati, A.K., 2012. Determining the Diagenetic Conditions of Concretion Formation: Assessing Temperatures and Pore Waters Using Clumped IsotopesCURRENT RIPPLES. Journal of Sedimentary Research 82, 1006-1016.

Marin, J., Chaussidon, M., Robert, F., 2010. Microscale oxygen isotope variations in 1.9Ga Gunflint cherts: Assessments of diagenesis effects and implications for oceanic paleotemperature reconstructions. Geochimica et Cosmochimica Acta 74, 116-130.

Muehlenbachs, K., 1998. The oxygen isotopic composition of the oceans, sediments and the seafloor. Chem. Geol. 145, 263-273.

Muehlenbachs, K., Clayton, R.N., 1976. Oxygen isotope composition of the oceanic crust and its bearing on seawater. Journal of Geophysical Research 81, 4365-4369.

Murata, K.J., Friedman, I., Gleason, J.D., 1977. Oxygen isotope relations between diagenetic silica minerals in Monterey Shale, Temblor Range, California. American Journal of Science 277, 259-272.

Pack, A., Herwartz, D., 2014. The triple oxygen isotope composition of the Earth mantle and understanding Delta O-17 variations in terrestrial rocks and minerals. Earth and Planetary Science Letters 390, 138-145.

Passey, B.H., Henkes, G.A., 2012. Carbonate clumped isotope bond reordering and geospeedometry. Earth and Planetary Science Letters 351-352, 223-236.

Perry, E.C., 1967. The oxygen isotope chemistry of ancient cherts. Earth and Planetary Science Letters 3, 62-66.

Perry, E.C., Lefticariu, L., 2014. 9.5 - Formation and Geochemistry of Precambrian Cherts, in: Holland, H.D., Turekian, K.K. (Eds.), Treatise on Geochemistry (Second Edition). Elsevier, Oxford, pp. 113-139.

Ryb, U., Eiler, J.M., 2018. Oxygen isotope composition of the Phanerozoic ocean and a possible solution to the dolomite problem. Proceedings of the National Academy of Sciences 115, 6602-6607.

Schoenemann, S.W., Schauer, A.J., Steig, E.J., 2013. Measurement of SLAP2 and GISP $\delta^{17}O$ and proposed VSMOW-SLAP normalization for $\delta^{17}O$ and $^{17}O_{excess}$. Rapid Communications in Mass Spectrometry 27, 582-590.

Sengupta, S., Pack, A., 2018. Triple oxygen isotope mass balance for the Earth's oceans with application to Archean cherts. Chem. Geol.

Sharp, Z.D., Gibbons, J.A., Maltsev, O., Atudorei, V., Pack, A., Sengupta, S., Shock, E.L., Knauth, L.P., 2016. A calibration of the triple oxygen isotope fractionation in the SiO_2–H_2O system and applications to natural samples. Geochimica et Cosmochimica Acta 186, 105-119.

Sharp, Z.D., Wostbrock, J.A.G., Pack, A., 2018. Mass-dependent triple oxygen isotope variations in terrestrial materials. Geochemical Perspectives Letters 7, 27-31.

Stefurak, E.J.T., Fischer, W.W., Lowe, D.R., 2015. Texture-specific Si isotope variations in Barberton Greenstone Belt cherts record low temperature fractionations in early Archean seawater. Geochimica et Cosmochimica Acta 150, 26-52.

Stolper, D.A., Eiler, J.M., 2015. The kinetics of solid-state isotope-exchange reactions for clumped isotopes: A study of inorganic calcites and apatites from natural and experimental samples.

Tang, M., Chen, K., Rudnick, R.L., 2016. Archean upper crust transition from mafic to felsic marks the onset of plate tectonics. Science 351, 372-375.

Tartèse, R., Chaussidon, M., Gurenko, A., Delarue, F., Robert, F., 2017. Warm Archaean oceans reconstructed from oxygen isotope composition of early-life remnants. Geochemical Perspectives Letters 3, 55-65.

Tice, M.M., Lowe, D.R., 2006. The origin of carbonaceous matter in pre-3.0 Ga greenstone terrains: A review and new evidence from the 3.42 Ga Buck Reef Chert. Earth-Science Reviews 76, 259-300.

Trower, E.J., Lowe, D.R., 2016. Sedimentology of the ~3.3Ga upper Mendon Formation, Barberton Greenstone Belt, South Africa. Precambrian Research 281, 473-494.

Valley, J.W., Kitchen, N., Kohn, M.J., Niendorf, C.R., Spicuzza, M.J., 1995. UWG-2, a garnet standard for oxygen isotope ratios: Strategies for high precision and accuracy with laser heating. Geochimica Et Cosmochimica Acta 59, 5223-5231.

Veizer, J., Bruckschen, P., Pawellek, F., Diener, A., Podlaha, O.G., Carden, G.A.F., Jasper, T., Korte, C., Strauss, H., Azmy, K., Ala, D., 1997. Oxygen isotope evolution of Phanerozoic seawater. Palaeogeography, Palaeoclimatology, Palaeoecology 132, 159-172.

Wallmann, K., 2004. Impact of atmospheric CO_2 and galactic cosmic radiation on Phanerozoic climate change and the marine δ18O record. Geochemistry, Geophysics, Geosystems 5, n/a-n/a.

Wostbrock, J.A.G., Sharp, Z.D., Sanchez-Yanez, C., Reich, M., van den Heuvel, D.B., Benning, L.G., 2018. Calibration and application of silica-water triple oxygen isotope thermometry to geothermal systems in Iceland and Chile. Geochimica et Cosmochimica Acta 234, 84-97.

Yeung, L.Y., Hayles, J.A., Hu, H., Ash, J.L., Sun, T., 2018. Scale distortion from pressure baselines as a source of inaccuracy in triple-isotope measurements. Rapid Communications in Mass Spectrometry 0.

Author contributions: The manuscript was written by Justin Hayles and Laurence Yeung. Field work was conducted by Justin Hayles, Asmita Banerjee, Bing Shen and Martin Homann. Oxygen isotope analysis was conducted by Justin Hayles. LA-ICPMS analysis was conducted by Justin Hayles and Hehe Jiang. All authors contributed to interpretations.

Competing interests: Authors declare no competing interests.;

Data and materials availability: All data is available in the main text or the supplementary materials.